# Physical Properties of Collective Motion in Suspensions of Bacteria

Andrey Sokolov and Igor S. Aranson

*Materials Science Division, Argonne National Laboratory, 9700 South Cass Avenue, Argonne, Illinois 60439, USA*

(Received 14 August 2012; published 14 December 2012)

A suspension of microswimmers, the simplest realization of active matter, exhibits novel material properties: the emergence of collective motion, reduction in viscosity, increase in diffusivity, and extraction of useful energy. Bacterial dynamics in dilute suspensions suggest that hydrodynamic interactions and collisions between the swimmers lead to collective motion at higher concentrations. On the example of aerobic bacteria *Bacillus subtilis*, we report on spatial and temporal correlation functions measurements of collective state for various swimming speeds and concentrations. The experiments produced a puzzling result: while the energy injection rate is proportional to the swimming speed and concentration, the correlation length remains practically constant upon small speeds where random tumbling of bacteria dominates. It highlights two fundamental mechanisms: hydrodynamic interactions and collisions; for both of these mechanisms, the change of the swimming speed or concentration alters an overall time scale.

DOI: 10.1103/PhysRevLett.109.248109 PACS numbers: 87.16.−b, 05.65.+b

A suspension of microswimmers is the simplest realization of active matter. It exhibits novel material properties, from the emergence of collective motion [1,2], reduction in viscosity [3], and increase in diffusivity [4,5] to the extraction of useful energy [6]. Swarming, one of the manifestations of collective motion in suspensions of motile microorganisms, is critical for the survival of the colonies and has a profound effect on the transport of nutrients, oxygen [5], signaling, and the formation of biofilms [7]. Suspensions of swimming bacteria have recently attracted enormous attention as a convenient experimental and theoretical model to examine fundamental aspects of collective motion [8,9] exhibited by various biological and synthetic systems, ranging from flocks of animals and cytoskeletal filaments to vibrated granular rods and chemical- and light-powered microswimmers [10–18]. While a large number of theoretical and experimental papers was published on various aspects of collective motion [1,2,19–27], the field lacks conceptual clarity, especially on the role of individual interactions between bacteria on the properties of collective motion. Studies of bacterial dynamics in dilute suspensions suggest that hydrodynamic interactions and collisions between the swimmers lead to collective motion at higher concentrations [9,21]. In spite of the fact that models based on pure hydrodynamic interactions were able to reproduce some key features of collective motion [19,20,22], like the instability of isotropic state at concentrations above critical, recent experimental and theoretical works highlighted the importance of direct collision and near-field hydrodynamic interaction between the swimmers [8,9,21].

We probe physical properties of collective motion in suspension of bacteria *Bacillus subtilis* via direct measurements of collective bacterial flow and its correlation length and time. We carried out a set of experiments where the swimming speed of aerobic bacteria was controlled by the concentration of dissolved oxygen. Clearly, the swimming speed and the concentration of bacteria, determining the total amount of energy injected by microorganisms into the suspending fluid, are fundamental parameters of the collective swimming state. Moreover, the magnitude of bacterial flow and the frequency of collisions between bacteria are proportional to their swimming speed and concentration. Thus, the variation of bacterial swimming speed and concentration provides a unique insight into the organization and structure of the collective motion in active suspensions. Our experiments produced a puzzling result: while the energy injection rate is proportional to the swimming speed and concentration, the correlation length remains practically constant upon small speeds where random tumbling of bacteria dominates. It highlights two fundamental mechanisms: hydrodynamic interactions and collisions; for both of these mechanisms, the change of the swimming speed or concentration only alters an overall time scale.

Experiments were performed on strain 1085 of *Bacillus subtilis*, a rod-shaped bacterium $\sim 5\ \mu$m long and $\sim 0.7\ \mu$m in diameter. The bacteria were grown in a Terrific Broth medium (Sigma T5574) in sealed vials under microaerobic conditions, resulting in colonies with increased resistance to oxygen starvation and overall higher swimming speed. Then the samples were concentrated by centrifugation and placed in a fresh Terrific Broth medium at concentration $\sim 1$–$3 \times 10^{10}$ cm$^{-3}$. In the following, concentration is measured in units of $c_0$, where $c_0 = 8 \times 10^8$ cm$^{-3}$ is concentration of the bacteria in the stationary phase of growing.

The experimental apparatus is a modification of our custom-built automated cell [2,3,6]. The computer-controlled experimental cell based on of a free-standing

 

film of adjustable thickness design was placed inside a container mounted on the moving stage of an inverted microscope. A 10-$\mu$l drop of bacterial suspension was placed between two crossed pairs of fibers, which formed a small square "window." By moving the frame, the drop was stretched out until it formed a $5 \times 5$ mm free-standing film of thickness $\sim$400 $\mu$m. Average swimming speed of the bacteria was controlled by the amount of dissolved oxygen. A chamber with bacterial film was connected to cylinders of compressed air and nitrogen through two computer-controlled magnetic valves. The concentration of oxygen dissolved in the suspended liquid film was measured directly by a thin-wire sensor [28]. A novel feature of the apparatus is the possibility to change the oxygen-nitrogen ratio cyclically, with an adjustable rate.

Figure 1(a) shows swimming speed of bacteria vs oxygen concentration; up to 20 oxygen-nitrogen cycles were performed during a single experiment to accumulate sufficient statistics. Using particle image velocimetry (PIV), we have found that for a normal (atmospheric) oxygen fraction, the average speed of bacterial flow is of the order of 50–60 $\mu$m/s. Deprivation of oxygen reduces average swimming speed to 10 $\mu$m/s. On the basis of many measurements we observe that the speed of bacteria can be represented by a linear function of oxygen concentration.

We have found that at high concentrations, the bacteria respond almost immediately to the change in oxygen concentration by changing their swimming speed (see the Supplemental Material [29]). Aerobic bacteria tend to form a depletion layer in the middle of the film and accumulate near open surfaces due to oxygentaxis [5,30]. Since the experiment is performed in open thin-film geometry, the accumulation of bacteria near top or bottom surfaces was minor. Moreover, in our experiment the bacteria were also grown under microaerobic conditions, resulting in increased resistance to oxygen starvation. Thus, the formation of a depletion layer was not as pronounced as in Ref. [5]. The liquid film also shrinks in the course of the experiment due to water evaporation. However, it does not lead to a noticeable increase in the concentration [31].

We performed about 400 oxygen cycles at different rates, yielding change of the swimming speed with the rates from 0.4 $\mu$m/s$^2$ to 3 $\mu$m/s$^2$. The results were split into four approximately equal groups according to the rate of change: slow or fast increase and slow or fast decrease of swimming speed, see Fig. 1(b). The measured correlation length $L$ (spatial scale of collective motion) is practically constant at swimming speeds above 20 $\mu$m/s and falls off rapidly below it. The falloff is attributed to a competition between noise (due to tumbling of bacteria) and ordering dynamics. Since the correlation length $L$ is practically constant at swimming speeds above 20 $\mu$m/s, we argue that the effect of noise on collective motion is negligible, while at swimming speeds below 20 $\mu$m/s, noise significantly affects bacterial dynamics, tending to terminate the collective motion. Corresponding images demonstrating bacterial flow for different oxygen contents (or swimming speeds) are shown in Figs. 2(a)–2(d). Despite the fact that the average swimming speed changes by a factor of 3, no visible change in the flow pattern is observed in Figs. 2(a)–2(c). For small swimming speeds [Fig. 2(d)] correlation length

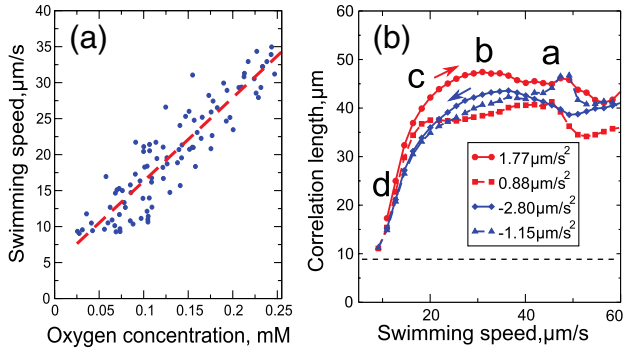


FIG. 1 (color online). (a) Dependence of average swimming speed of bacteria at high concentration (collective regime) on the concentration of oxygen; blue heavy dots are experimental measurements, and dashed line is a guide for the eye. (b) Correlation length as a function of swimming speed for different speed change rates. The arrows indicate the direction of the change in swimming speed. Dashed line depicts size of PIV interrogation window.

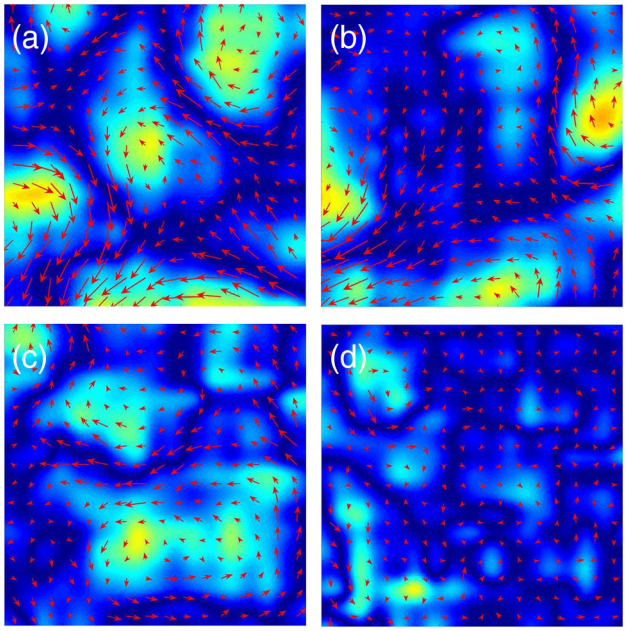


FIG. 2 (color online). Select images illustrating instant flow pattern at the bottom of the film for different concentrations of oxygen (or average swimming speeds); red arrows depict the direction and magnitude of bacterial flow, and colors show the vorticity magnitude of bacterial flow. Concentration of bacteria $c = 30c_0$. The corresponding swimming speeds are indicated in Fig. 1(b) by letters a–d, see also Supplemental Material [29], movies 1 and 2.

decreases and the flow becomes more disordered compared to Figs. 2(a)–2(c) [32].

Temporal properties of the collective state, characterized by the velocity's time autocorrelation functions, $K(t)$, were examined for different swimming velocities and concentrations, Figs. 3(a) and 3(c). In the regime of collective swimming, the functions (except the curve in Fig. 3(c) for $c = 9.5c_0$, which is below the threshold of collective motion $c_{cr} \approx 12c_0$) exhibit reasonable collapse if the time is renormalized by $t_0 = 1/Vcl^2$, where $V$ is average swimming speed, $c$ is concentration of bacteria, and

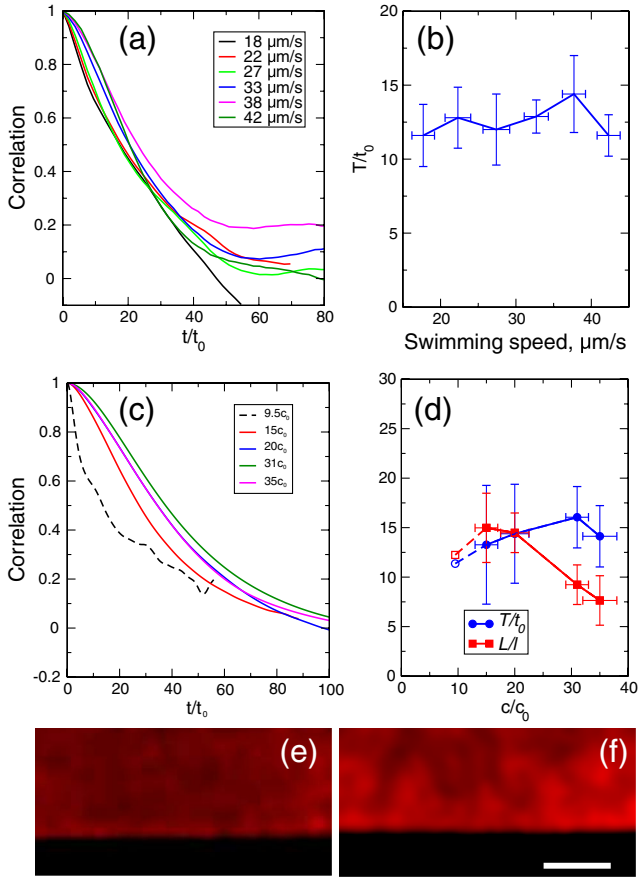


FIG. 3 (color online). (a) Velocity's time autocorrelation functions at different average swimming speed values $V$. Time is scaled by mean free time $t_0 = 1/cVl^2$. Concentration of bacteria is $30c_0$ (b) Normalized correlation time $T$ (scaled by $t_0 = 1/cVl^2$) for different values of swimming speed. (c) Velocity's time autocorrelation functions scaled by $t_0$ for different concentrations. Average swimming speed $\approx 39$ $\mu$m/s. Collective behavior disappears at concentration $\approx 12c_0 \sim 10^9$ cm$^{-3}$ (d) Correlation time $T$ (scaled by $t_0 = 1/cVl^2$) and spatial correlation length $L$ (scaled by size of bacterium $l$) for different values of bacterial concentration. Open symbols mark concentration $9.5c_0$ where no collective motion is observed. Vertical optical coherence tomography (OCT) scans of the bottom part of the film for concentrations $c = 15c_0$ (e) and $c = 30c_0$ (f). Bioconvection on the panel (f) is manifested by bright plumes of increased bacterial concentration. Scale bar is 225 $\mu$m.

$l = 5$ $\mu$m is typical length of a bacterium. Note that $t_0$ has a meaning of the mean free time between collisions in kinetic theory of gases. Deviations from the master curve are possibly related to finite size effects and the onset of bioconvection, compare Figs. 3(e) and 3(f) [5,30]. Far from the threshold, the correlation time normalized on $t_0$ and the spatial correlation length $L$ show practically no dependence on the velocity, Fig. 3(b). We believe that a decrease in the correlation length in Fig. 3(d) can be related to the following effects: increased tumbling rate due to lack of nutrients or oxygen in the bulk of the film, onset of bioconvection, slowdown of bacteria after collisions, jamming, etc.; see Fig. 3(f). Since tracking of individual bacteria at high concentrations is a technically difficult problem, we were not able to measure the tumbling rate as a function of concentration and provide a detailed analysis of these mechanisms.

To quantify the effect of tumbling, the dominant source of rotational noise, experiments were performed in a dilute regime, well below the threshold of collective swimming, where each and every bacterium was tracked individually [see Figs. 4(a) and 4(b) and Supplemental Material [29], movies 3 and 4). While at a low oxygen concentration, the tracks of individual bacteria resemble random walk [Fig. 4(a)], at higher concentration the tracks became mostly straight lines [Fig. 4(b)]. There are two major contributions to the rotational noise: fluctuations of bacteria orientations and fluctuations of their velocity vectors: both exhibit similar trends versus swimming speed. In the following we characterize noise via fluctuations of the velocities. Figure 4(c) depicts the magnitude of angular velocity averaged over all bacteria in each frame versus swimming speed. Finite values for high velocities are due to the rotation of flagella and counterrotation of the bacterial body, which is present even for straight swimming, where the tumbling rate is low. Noticeable hysteresis occurs in each oxygen cycle: value is higher for the transition from fast swimming to slow at the same swimming speed. That explains the hysteresis at high speed change rates (Fig. 1(b), solid lines), while for low rate (Fig. 1(b), dashed lines) the hysteresis is absent. The origin of hysteresis is likely related to a complex biochemical response of bacteria on the change of oxygen concentration. The tumbling rate, characterized by rational diffusion $D$, versus swimming speed is shown in Fig. 4(d). The plot depicts the distribution of rotational diffusion extracted from tracks of all bacteria in the frame; there is a clear trend towards the decrease of the tumbling rate with the increase of swimming speed due to the increase in oxygen concentration.

Two mechanisms, alignment via collisions and hydrodynamic interactions, are controlled by the bacterial swimming speed $V$ and concentration $c$. Our experiments (see also Ref. [2]) revealed that the correlation length $L$ is about 5–10 bacterial length and above the threshold concentration and speed practically stayed constant, see Figs. 1(b)

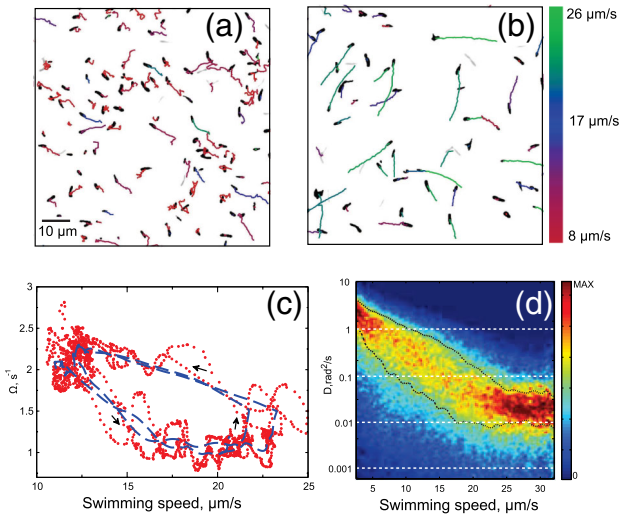


FIG. 4 (color online). Tumbling of *Bacillus subtilis* at low concentrations. (a,b): Tracks of individual bacteria for different oxygen concentrations; color represents average swimming speed for the last 1.2 s according to color bar on the right. At low oxygen concentration (a), the tracks resemble random walk. Increasing oxygen concentration (b) results in an increase of straight-swimming fraction. (c) Magnitude of angular velocity vs swimming speed averaged over all bacteria in the field of view with 0.5-s time interval; two oxygen cycles are shown. Red heavy dots depict experimental values, dashed blue line shows running average. The direction is shown by black arrows. (d) Probability distribution of rotational diffusion $D$ obtained from $2 \times 10^5$ independent tracks in the range of swimming speeds. Two dashed black lines indicate boundaries with the probability above 50% for each speed value. See also Supplemental Material [29], movies 3 and 4.

and 3. It suggests that far from the threshold the correlation length $L$ is entirely determined by properties of the swimmers: their size (possibly including length of flagella) and shape. To estimate $L$, consider the evolution of a nucleus of radius $R$ formed by bacteria oriented in $x$ direction and immersed in a "sea" of randomly swimming bacteria. The nucleus expands due to alignment of nearby bacteria via collisions and is deformed by a flow created by other bacteria [29]. We assume for simplicity that the alignment is instant, and after a collision the nucleus size increases by the length of a bacterium $l$. Since the time between collisions is of the order of mean free time $t_0 = 1/cl^2V$, the speed of nucleus expansion is $V_c \sim l/t_0 = cl^3V$ (compare to Fisher wave propagating into unstable state [33]).

Since the Reynolds number of an individual bacterium is exceedingly small, the flow is described by the linear Stokes equation [34,35]. For a bacterium swimming in $x$ direction, the flow can be approximated by a hydrodynamic dipole, $\mathbf{u}(\mathbf{r}) = p\mathbf{r}(3x^2/r^2 - 1)/8\pi r^3$, where $r = |\mathbf{r}|$ is the distance vector relative to the center of dipole, $p = aVl^2$ is the dipole strength, and $a$ is the constant determined by the shape-aspect ratio. For example, for *Escherichia coli*, the dipole moment is $p \approx 32\ \mu\text{m}^3/\text{s}$ yielding $a \approx 0.1$–$0.2$ [8]. Bacteria in the nucleus create a flow at $r = R$ with the magnitude $V_h \sim cpR$; the flow expands the nucleus in $x$ direction and contracts it in transverse directions. Equating the hydrodynamic contractile velocity $V_h$ and nucleus expansion rate $V_c$ yields a critical radius, $R \sim cl^3V/cp = l/a \approx 5$–$10l$, i.e., the order 5–10 bacterial length, independent of the swimming speed and concentration, in agreement with our experimental observations. This estimate is valid for not too high concentrations when the collisions still can be treated as binary and the flow as a superposition of point dipoles.

The decrease of correlation length at small swimming speeds can be attributed to the effect of random tumbling dominating the collective behavior. In Ref. [2] the phase transition to collective swimming is described by an order parameter $\psi$ characterizing local alignment between the bacteria. The order parameter is nonzero for concentrations $c$ exceeding the critical concentration $c_c$, $\psi^2 \sim \sqrt{c - c_c}$, and the correlation length $L$ is a monotonic function of $\psi$. The critical concentration $c_c$ increases with the increase of the tumbling rate [9,22]: more concentrated suspension is needed to suppress randomness produced by tumbling. Rescaling time by a factor $V$ is equivalent to renormalization of the noise intensity by a factor of $1/V$ (see also Ref. [29]). Thus, the decrease of swimming speed $V$ leads to an effective increase of critical concentration, and, consequently, to the decrease of the correlation length $L$, as it is observed in the experiment.

In conclusion, we have shown that far from the threshold, the correlation length of collective motion is practically independent of the energy injection rate. It highlights two fundamental physical mechanisms determining the physical properties of collective motion: long-range hydrodynamic interactions and short-range collisions. Both mechanisms have similar scaling with the swimming speed and concentration of the bacteria. It hints that the correlation length is determined only by the shape and the size of the swimmer. Apart from the relevance to a broad class of active matter based on biological or synthetic self-propelled elements [10,11], our findings are crucial for further development of biomechanical systems utilizing the collective motion of subunits to achieve useful functions [6,10,12].

The work of I. S. A. and A. S. was supported by the U.S. Department of Energy, Office of Basic Energy Sciences, Division of Materials Science and Engineering, under Contract No. DEAC02-06CH11357.

[1] C. Dombrowski, L. Cisneros, S. Chatkaew, R. E. Goldstein, and J. O. Kessler, Phys. Rev. Lett. **93**, 098103 (2004).

[2] A. Sokolov, I. S. Aranson, J. O. Kessler, and R. E. Goldstein, Phys. Rev. Lett. **98**, 158102 (2007).

[3] A. Sokolov and I. S. Aranson, Phys. Rev. Lett. **103**, 148101 (2009).
[4] X.-L. Wu and A. Libchaber, Phys. Rev. Lett. **84**, 3017 (2000).
[5] A. Sokolov, R. E. Goldstein, F. I. Feldchtein, and I. S. Aranson, Phys. Rev. E **80**, 031903 (2009).
[6] A. Sokolov, M. M. Apodaca, B. A. Grzybowski, and I. S. Aranson, Proc. Natl. Acad. Sci. U.S.A. **107**, 969 (2010).
[7] M. F. Copeland and D. B. Weibel, Soft Matter **5**, 1174 (2009).
[8] K. Drescher, J. Dunkel, L. H. Cisneros, S. Ganguly, and R. E. Goldstein, Proc. Natl. Acad. Sci. U.S.A. **108**, 10 940 (2011).
[9] I. S. Aranson, A. Sokolov, J. O. Kessler, and R. E. Goldstein, Phys. Rev. E **75**, 040901(R) (2007).
[10] R. Dreyfus, J. Baudry, M. L. Roper, M. Fermigier, H. A. Stone, and J. Bibette, Nature (London) **437**, 862 (2005).
[11] W. F. Paxton, A. Sen, and T. Mallouk, Chem. Eur. J. **11**, 6462 (2005).
[12] A. Snezhko and I. S. Aranson, Nat. Mater. **10**, 698 (2011).
[13] I. D. Couzin, J. Krause, N. R. Franks, and S. A. Levin, Nature (London) **433**, 513 (2005).
[14] V. Schaller, C. Weber, C. Semmrich, E. Frey, and A. R. Bausch, Nature (London) **467**, 73 (2010).
[15] S. Köhler, V. Schaller, and A. R. Bausch, Nat. Mater. **10**, 462 (2011).
[16] Y. Sumino, K. H. Nagai, Y. Shitaka, D. Tanaka, K. Y. Yoshikawa, H. Chate, and K. Oiwa, Nature (London) **483**, 448 (2012).
[17] A. Kudrolli, G. Lumay, D. Volfson, and L. S. Tsimring, Phys. Rev. Lett. **100**, 058001 (2008).
[18] M. Ibele, T. E. Mallouk, and A. Sen, Angew Chem Int Ed Engl. **48**, 3308 (2009).
[19] D. Saintillan and M. J. Shelley, Phys. Rev. Lett. **99**, 058102 (2007).
[20] D. Saintillan and M. J. Shelley, Phys. Rev. Lett. **100**, 178103 (2008).
[21] L. H. Cisneros, J. O. Kessler, S. Ganguly, and R. E. Goldstein, Phys. Rev. E **83**, 061907 (2011).
[22] D. L. Koch and G. Subramanian, Annu. Rev. Fluid Mech. **43**, 637 (2011).
[23] J. P. Hernandez-Ortiz, C. G. Stoltz, and M. D. Graham, Phys. Rev. Lett. **95**, 204501 (2005).
[24] P. T. Underhill, J. P. Hernandez-Ortiz, and M. D. Graham, Phys. Rev. Lett. **100**, 248101 (2008).
[25] C. W. Wolgemuth, Biophys. J. **95**, 1564 (2008).
[26] X. Chen, X. Dong, A. Beér, H. L. Swinney, and H. P. Zhang, Phys. Rev. Lett. **108**, 148101 (2012).
[27] T. Ishikawa, N. Yoshida, H. Ueno, M. Wiedeman, Y. Imai, and T. Yamaguchi, Phys. Rev. Lett. **107**, 028102 (2011).
[28] The following method was used to monitor oxygen concentration. Two thin steel wires, diameter 100 $\mu$m, were submerged in the film next to two opposite supporting fibers, but remained in the proximity of open surface. The concentration of dissolved oxygen was monitored by the transmission of an electrical current through the bacterial suspension: the cathode produced a measurable electrical current at constant polarizing voltage directly proportional to the partial pressure of oxygen. Electrical resistance was processed by LabView in real time and the required commands were sent to magnetic valves, controlling oxygen and nitrogen feeding rates. Two reference points were used for calibration: maximal current corresponding to concentration of dissolved oxygen in water equilibrated with air, which is 0.25 mM, and minimal current corresponding to zero oxygen concentration, see L. C. Clark, Jr., R. Wolf, D. Granger, and Z. Taylor, J. Appl. Physiol. **6**, 189 (1953).
[29] See Supplemental Material at http://link.aps.org/supplemental/10.1103/PhysRevLett.109.248109 for supplementary information and auxiliary files containing experimental movies.
[30] T. J. Pedley and J. O. Kessler, Annu. Rev. Fluid Mech. **24**, 313 (1992).
[31] The free-standing film is significantly thinner in the center. As a result, the total volume of the liquid film decreases much slower than film thickness in the center. It was confirmed by the Optical Coherence Tomography (OCT), see supplement [29] illusrating that the change in oxygen concentration and evaporation does not noticeably affect the distribution of bacteria in the observation window.
[32] The outcome of PIV is not very accuarate when the correlation length $L$ becomes comparable with the size of a bacterium due to limitations of the optical flow detection of multiple overlapping bacteria moving in random directions. We anticipate that for swimming speeds below 10 $\mu$m/s the correlation length asymptotically approaches a value of the order of the bacterial size.
[33] A. Kolmogorov, I. Petrovskii, and N. Piscounov, *A study of the Diffusion Equation with Increase in the Amount of Substance, and its Application to a Biological Problem*. edited by V. M. Tikhomirov, Selected Works of A. N. Kolmogorov (Kluwer, 1991), pp. 248–270. Translated by V. M. Volosov, Bull. Moscow Univ., Math. Mech **1**, 1 (1937).
[34] E. Lauga and T. R. Powers, Rep. Prog. Phys. **72**, 096601 (2009).
[35] E. M. Purcell, Am. J. Phys. **45**, 3 (1977).